

# Ocean acoustic interferometry

Laura A. Brooks<sup>a)</sup> and Peter Gerstoft

Marine Physical Laboratory, Scripps Institution of Oceanography, La Jolla, California 92093

(Received 12 January 2007; revised 13 March 2007; accepted 16 March 2007)

Ocean acoustic interferometry refers to an approach whereby signals recorded from a line of sources are used to infer the Green's function between two receivers. An approximation of the time domain Green's function is obtained by summing, over all source positions (stacking), the cross-correlations between the receivers. Within this paper a stationary phase argument is used to describe the relationship between the stacked cross-correlations from a line of vertical sources, located in the same vertical plane as two receivers, and the Green's function between the receivers. Theory and simulations demonstrate the approach and are in agreement with those of a modal based approach presented by others. Results indicate that the stacked cross-correlations can be directly related to the shaded Green's function, so long as the modal continuum of any sediment layers is negligible. © 2007 Acoustical Society of America. [DOI: 10.1121/1.2723650]

PACS number(s): 43.30.Yj, 43.30.Gv, 43.60.Ac [AIT]

Pages: 3377–3385

## I. INTRODUCTION

Approximation of the Green's function between two points in both open and closed environments has been a subject of interest over the last few years. Lobkis and Weaver<sup>1</sup> showed, both theoretically and experimentally, that the Green's function between two points can be determined from their temporal cross-correlation within a diffuse ultrasonic field. This concept was extended by Derode *et al.*<sup>2</sup> who showed that the Green's function can be conditionally recovered in an open scattering medium. They concluded that although the Green's function can be determined from cross-correlations from a single source within a lossless closed cavity in which it is assumed that the eigenmodes do not degenerate, the Green's function will only emerge from cross-correlations within an open scattering medium if the cross-correlations are summed over a perfect time-reversal mirror. Wapenaar<sup>3</sup> and Van Manen *et al.*<sup>4</sup> demonstrated that retrieval of the Green's function through summed cross-correlations can also be achieved in an inhomogeneous medium. Sánchez-Sesma *et al.* presented the canonical problem of elastodynamic Green's function retrieval in a homogeneous medium<sup>5</sup> and in an infinite space with a cylinder inclusion.<sup>6</sup> They showed that the Fourier transform of the mean cross-correlation of motion between two points is proportional to the imaginary part of the corresponding exact Green's tensor, provided that there is equipartitioning of energy.

Extraction of the Green's function by cross-correlation from ultrasonic noise,<sup>7–9</sup> ambient noise in a homogeneous medium,<sup>10</sup> ambient ocean acoustic noise,<sup>11–14</sup> seismic noise,<sup>15–20</sup> helioseismic noise,<sup>21</sup> and even moon-seismic noise<sup>22</sup> has been undertaken, and the governing concepts are now quite well understood.

Three papers are of particular relevance to this work. Using a modal approach, Roux and Fink<sup>23</sup> showed theoretically in the frequency domain and through simulation that

the Green's function between two points in a waveguide can be determined by summing the cross-correlations from a vertical line of sources that are located in the same plane as the two receivers, external to the two receivers. Sabra *et al.*<sup>12</sup> used a stationary phase argument to formulate the time domain Green's function for time-averaged surface generated ambient noise cross-correlation, where the sources were modeled as a horizontal plane of point sources at a constant depth. Also using the method of stationary phase, Snieder *et al.*<sup>24</sup> presented a formulation that suggests that seismic interferometry using sources equally spaced along the surface of a homogeneous medium, with a horizontal reflector and no free surface, in the same vertical plane as two receivers located within said medium, can be used to determine the Green's function between the two receivers. They showed that when multiple bottom reflectors are included, spurious multiples may occur due to the region of interest not being completely enclosed by sources, and concluded that, theoretically, these spurious multiples could be removed by including an additional set of sources below the reflectors.

Within this paper, the relationship between cross-correlations from a vertical line of active sources to two receivers within a waveguide, and the shaded time domain Green's function between said receivers, is explored. We call this approach ocean acoustic interferometry (OAI), as it is related to classical and seismic interferometry,<sup>25</sup> where interferometry refers to the determination of information from the interference phenomena between pairs of signals. The method of stationary phase is applied to simple reflective environments, providing an alternative theoretical means of describing and understanding the physics governing the cross-correlation of such a source configuration, and how this can be used to extract an amplitude shaded time domain Green's function. This work is distinct from work presented by Roux and Fink,<sup>23</sup> Sabra *et al.*,<sup>12</sup> and Snieder *et al.*,<sup>24</sup> in that a stationary phase derivation is applied to a column of sources in a waveguide. A detailed physical and mathematical discussion of spurious arrivals obtained in connection with OAI is presented. Numerical simulations of these envi-

<sup>a)</sup>Also at the School of Mechanical Engineering, University of Adelaide, Australia; electronic mail: lbrooks@mecheng.adelaide.edu.au

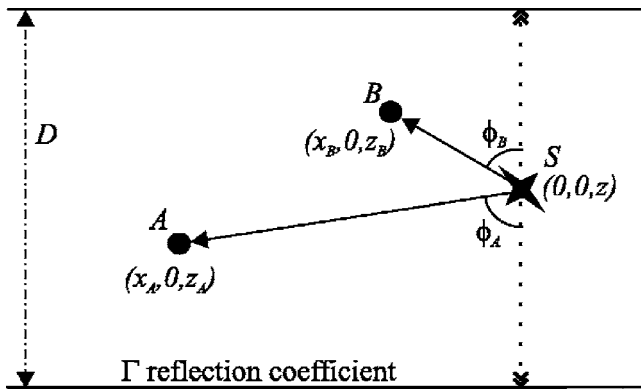


FIG. 1. Source-receiver geometry and notation: the source  $S$  is located at  $(0, 0, z)$ , and receivers  $A$  and  $B$  are located at  $(x_A, 0, z_A)$  and  $(x_B, 0, z_B)$ , respectively, within a waveguide of depth  $D$ .

ronments support the theory. A refractive environment with more realistic water column, sediment, and bottom parameters is also analyzed through numerical simulations. These geometrically simple scenarios are chosen as they allow for understanding of the results, but the underlying concepts are applicable to complex environments. Both the unstacked cross-correlations as a function of depth and the stacked cross-correlations are analyzed. The effect of limiting the sources to the water column is discussed and it is shown that the accuracy of OAI increases if the source column is extended through the sediment. The spurious arrivals obtained here are compared with those obtained by Sabra *et al.*<sup>12</sup> and Snieder *et al.*<sup>24</sup> The manifestations of these aberrations are distinct in each case and these differences are explained by considering the different environments and geometrical setup used.

## II. THEORY

Consider the waveguide depicted in Fig. 1. The  $x$ ,  $y$ , and  $z$  directions are defined as the horizontal axis, the axis in-and-out of the page, and the vertical axis, respectively. A vertical plane of sources spanning the water column (i.e., the  $z$  direction) and extended in the  $y$  direction would form a perfect time-reversal mirror, meeting the requirements for determination of the Green's function between two points via cross-correlation methods.<sup>2</sup> However, it has previously been shown that only sources in the same vertical plane as the two receivers will contribute significantly to the correlation integral.<sup>12,24</sup> A vertical line of sources is therefore uniformly and densely distributed within the vertical plane containing receivers  $A$  and  $B$ , external to the two receivers, and closer to  $B$ . The sum of the cross-correlations of the signals received at  $A$  and  $B$  (adapted from Ref. 24) in the frequency domain is

$$C_{AB}(\omega) = |\rho_s S(\omega)|^2 n \int_0^D G(\mathbf{r}_A, \mathbf{r}_S) G^*(\mathbf{r}_B, \mathbf{r}_S) dz, \quad (1)$$

where  $\rho_s$  is the density at the source,  $S(\omega)$  is the source spectrum,  $n$  is the number of sources per unit length,  $G(\mathbf{r}_\psi, \mathbf{r}_S)$  is the Green's function between the source  $S$  and receiver  $\psi$ , and  $*$  denotes complex conjugation. The lower bound of the integral is 0 since the waveguide has a free surface at  $z=0$  and the upper bound is the waveguide depth

$D$  since there are no reflective surfaces below this depth. This summed cross-correlation can, in the time domain, be determined from real or simulated data by calculating the cross-correlation for each source depth and then summing (also known as "stacking") the result. The sum of the cross-correlations is related to the Green's function between  $A$  and  $B$ . This relationship is derived here for reflective environments using the method of stationary phase.

The 3D Green's function within a homogeneous medium is

$$G_f(R) = \frac{e^{ikR}}{4\pi R}, \quad (2)$$

where  $k$  is the wave number and  $R$  is the distance from the source. The full Green's function at each receiver can be written as the superposition of the direct and reflected waves. If the medium is an isovelocity waveguide, bounded above by a free surface and below by a reflective bottom with reflection coefficient  $\Gamma$ , the Green's function between the source  $S$  and receiver  $\psi$  is written in terms of the waveguide and source-receiver geometry<sup>26</sup> as

$$G(\mathbf{r}_\psi, \mathbf{r}_S) = \sum_{b_\psi=0}^{\infty} \Gamma^{b_\psi} G_f(\sqrt{x_\psi^2 + (2b_\psi D + z \pm z_\psi)^2}) + \sum_{b_\psi=1}^{\infty} \Gamma^{b_\psi} G_f(\sqrt{x_\psi^2 + (2b_\psi D - z \pm z_\psi)^2}), \quad (3)$$

where  $b_\psi$  is the number of bottom bounces for a given path and  $D$  is the depth of the waveguide. The first term on the rhs includes all upgoing waves and the second term includes all downgoing waves as measured from the source.

Inserting Eq. (3) into Eq. (1) yields an expression for the correlation that consists of the sum of the integrals of all possible combinations of the interaction between any path to the first receiver and any path to the second. Although the cross-correlation includes the sum of all path interactions, each path interaction can be analyzed separately and summed together at the end to yield the complete solution. Hence, only one of these individual interactions is considered here. Substitution of Eq. (2) into Eq. (1) (i.e., cross-correlation between two arbitrary paths) yields

$$I = \frac{\Gamma^{b_A+b_B}}{(4\pi)^2} \int \frac{e^{ik(L_A-L_B)}}{L_A L_B} dz, \quad (4)$$

where  $b_\psi$  is the number of bottom bounces for the path to receiver  $\psi$ , and  $L_\psi = \sqrt{x_\psi^2 + (2b_\psi D \pm z \pm z_\psi)^2}$  is the length of the given path between the source  $S$  and receiver  $\psi$ . The sign in front of  $z$  is positive when the wave departing the source is upgoing and negative when it is downgoing. Similarly, the sign in front of  $z_\psi$  is positive when the wave arriving at the receiver is downcoming and negative when it is upcoming.

### A. Stationary phase evaluation

Since  $1/(L_A L_B)$  varies slowly and the phase  $k(L_A - L_B)$  varies quickly within the region of interest, rapid oscillations of  $e^{ik(L_A - L_B)}$  over the integrand allow for the integral, Eq. (4), to be solved via the method of stationary phase.<sup>27</sup> Similar

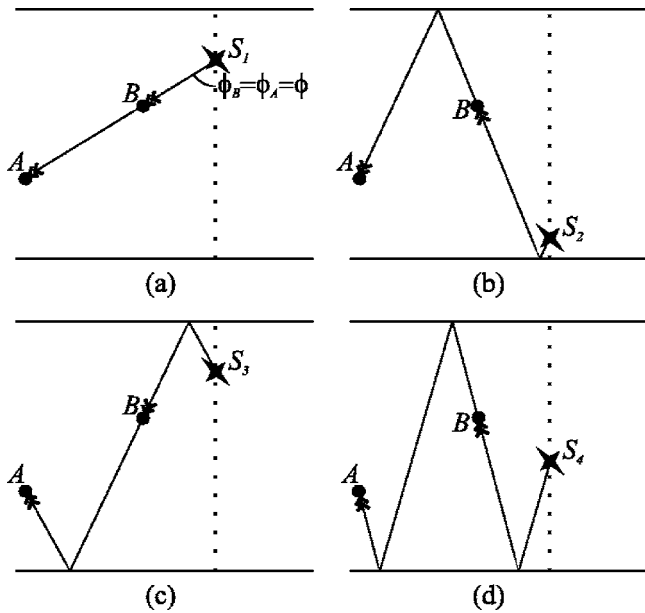


FIG. 2. Examples of wave paths that correspond to stationary points ( $\phi_A = \phi_B = \phi$ ): (a) direct wave, (b) surface reflected wave, (c) bottom reflected wave, and (d) surface and bottom reflected wave, between the receivers.

interferometric integrals have been solved by others.<sup>12,16,24</sup> We follow the idea of Snieder *et al.*, but assume a vertical rather than horizontal line of sources, and also extend the theory to a waveguide.

The stationary points of the integrand are found by evaluating the partial  $z$  derivative of the phase term and setting this to equal zero. The phase term is

$$L = L_A - L_B = \sqrt{x_A^2 + (2b_A D + \alpha_A z \pm z_A)^2} - \sqrt{x_B^2 + (2b_B D + \alpha_B z \pm z_B)^2}, \quad (5)$$

where  $\alpha_{\psi} = 1$  denotes an upgoing wave and  $\alpha_{\psi} = -1$  denotes a downgoing wave, as measured from the source. The partial differential with respect to  $z$  is

$$\frac{\partial L}{\partial z} = \alpha_A \left( \frac{2b_A D + \alpha_A z \pm z_A}{L_A} \right) - \alpha_B \left( \frac{2b_B D + \alpha_B z \pm z_B}{L_B} \right). \quad (6)$$

Writing Eq. (6) in terms of the acute angle  $\phi_{\psi}$  between the path and the vertical, at the point of departure from the source (see Fig. 1), yields

$$\frac{\partial L}{\partial z} = \alpha_A \cos \phi_A - \alpha_B \cos \phi_B. \quad (7)$$

Setting the partial  $z$  derivative to zero yields  $\phi_A = \phi_B$  when  $\alpha_A = \alpha_B$  (i.e., both waves depart as either upgoing or downgoing), and  $\phi_A = \pi - \phi_B$  when  $\alpha_A = -\alpha_B$  (i.e., one wave departs as upgoing and the other as downgoing). Since both  $\phi_A$  and  $\phi_B$  are less than  $\pi/2$ , the latter equation has no solutions. Thus a stationary point will only occur when both signals depart the source at the same angle. Therefore, the path to the farther receiver passes through the closer receiver, as shown in Fig. 2 for four different paths (remember that the above derivation holds for any individual path interaction and that the overall cross-correlation includes the sum of all

path interactions). Not all path combinations will exhibit a stationary point; for example, the direct path to A and any boundary interacting path to B will never satisfy  $\phi_A = \phi_B$ .

The integral, Eq. (4), is rewritten within the region of a given stationary point  $z_s$  as

$$I(z_s) \approx \frac{\Gamma^{b_A+b_B}}{(4\pi)^2} \frac{1}{L_A(z_s)L_B(z_s)} \int_{-\infty}^{\infty} e^{ik(L_A(z)-L_B(z))} dz. \quad (8)$$

Realistically, the sources exist over the finite limit  $(0, D)$ ; however, extension of these limits to infinity is valid as virtual sources exist over an infinite limit. The phase term can be approximated as a truncated Taylor series within the neighborhood of any stationary point:

$$L(z) \approx L(z_s) + \frac{(z-z_s)^2}{2} \left( \frac{\partial^2 L}{\partial z^2} \Big|_{z=z_s} \right), \quad (9)$$

$$\frac{\partial^2 L}{\partial z^2} \Big|_{z=z_s} = \sin^2 \phi_s \left( \frac{1}{L_A(z_s)} - \frac{1}{L_B(z_s)} \right). \quad (10)$$

Substituting the phase term and its second derivative, at the stationary point, into the truncated Taylor series, Eq. (9), and rewriting the integral, Eq. (8), assuming that  $L_A(z_s) > L_B(z_s)$  (which is valid since the source is closer to B than to A), yields

$$I(z_s) = \frac{\Gamma^{b_A+b_B}}{(4\pi)^2} \frac{e^{ik(L_A(z_s)-L_B(z_s))}}{L_A(z_s)L_B(z_s)} \times \int_{-\infty}^{\infty} \exp \left( -ik \frac{(z-z_s)^2}{2} \xi \sin^2 \phi_s \right) d(z-z_s), \quad (11)$$

where  $\xi = (1/L_B(z_s) - 1/L_A(z_s))$ . Equation (11) is a Fresnel integral and can therefore be solved by making the substitution  $k[(z-z_s)^2/2]\xi \sin^2 \phi_s = (\pi/2)\tau^2$ :

$$I(z_s) = \frac{\Gamma^{b_A+b_B}}{(4\pi)^2} \frac{e^{ik(L_A(z_s)-L_B(z_s))}}{L_A(z_s)L_B(z_s)} \times 2 \sqrt{\frac{\pi}{k\xi \sin^2 \phi_s}} \int_0^{\infty} \exp \left( -i \frac{\pi}{2} \tau^2 \right) d\tau = e^{i(3\pi/4)} \frac{\Gamma^{b_A+b_B}}{\sin \phi_s} \sqrt{\frac{\xi}{8k\pi}} G_f(R(z_s)), \quad (12)$$

where  $R(z_s) = L_A(z_s) - L_B(z_s)$  is the path length between A and B. Inclusion of the source factor,  $n|\rho_s S(\omega)|^2$ , and the relationship  $k = \omega/c$ , yields

$$C_{AB}(\omega) = \sum_{z_s} n|\rho_s S(\omega)|^2 I(z_s) = e^{i(3\pi/4)} n|S(\omega)|^2 \times \sum_{z_s} \left( \frac{\Gamma^{b_A+b_B} \rho_s^2 G_f^2(R(z_s))}{\sin \phi_s} \sqrt{\frac{\xi c}{8\pi\omega}} \right), \quad (13)$$

where the summation is over all stationary points.

Cross-correlation of the signals received from a vertical column of sources located in the same vertical plane as the receivers can therefore be seen to produce an amplitude and phase shaded Green's function. The amplitude shading consists of constant, path dependent, and frequency dependent components, while the phase shading is simply a  $3\pi/4$  phase

shift. If the summed cross-correlations are multiplied by  $e^{-i(3\pi/4)}$ , phase information, and hence travel times, of the  $|S(\omega)|^2/\sqrt{\omega}$  shaded Green's function can be determined. It will, however, be difficult to obtain the correct amplitudes since  $\Gamma^{b_A+b_B}$ ,  $\phi_s$ , and  $\xi = \sqrt{1/L_B(z_s) - 1/L_A(z_s)}$  are all path dependent.

The cross-correlation equation, Eq. (13), is in this particular form due to the mismatch between a 3D Green's function and a 1D source distribution (as commented by Snieder *et al.*<sup>24</sup>). If a 2D plane instead of the 1D column of sources were used, Eq. (1) would be a double integral spanning both the  $z$  and  $y$  directions, which could be solved as a product of two stationary phase integrals. If either a 2D plane of sources or the far-field approximation of the 2D Green's function,  $G(R) = e^{ikr}/\sqrt{r}$ , were incorporated, there would not be a dimensionality mismatch, and the sum of the cross-correlations, Eq. (13), would be

$$\tilde{C}_{AB}(\omega) = -in|S(\omega)|^2 \sum_{z_s} \left( \frac{\Gamma^{b_A+b_B} \rho_s^2 G_f(R(z_s))}{\sin \phi_s} \times \frac{c}{2\omega} \right), \quad (14)$$

where  $n$  is the number of sources per unit surface area for the plane of sources or the number of sources per unit length for the column of sources. Note that there is now no term (apart from the Green's function) containing  $L_A(z_s)$  and  $L_B(z_s)$  and therefore the amplitude shading is only dependent on the travel path through the  $\Gamma^{b_A+b_B}$  and  $\sin \phi_s$  terms.

The  $1/\omega$  factor in Eq. (14) means that the time domain Green's function is proportional to the derivative of the summed cross-correlations.<sup>10,12,16</sup> Due to a mismatch between the source dimensions and the Green's function, there is only a factor of  $1/\sqrt{\omega}$  in Eq. (13). The time domain Green's function is therefore proportional to a fractional derivative of the summed cross-correlation.<sup>24</sup>

## B. Incorporation of sediment layers

When the water column is bounded by fully reflective boundaries, as assumed for the preceding derivation, all of the energy is contained within the water column and truncation of the cross-correlation integral in Eq. (1) is avoided. The addition of sediment layers can cause truncation errors since the true integral will then extend to infinity (or at least to the basement) to account for sound that interacts with the sediment:

$$C_{AB}(\omega) = |\rho_s S(\omega)|^2 n \int_0^\infty G(\mathbf{r}_A, \mathbf{r}_S) G^*(\mathbf{r}_B, \mathbf{r}_S) dz. \quad (15)$$

If the source column is restricted to the water, the calculated integral still ceases at  $D$  and the stacked cross-correlations may vary from the frequency and phase shaded Green's function. As an example, consider a (purely theoretical) reflective environment, with constant sound speed, consisting of a water column and  $M$  sediment layers. The length of any path between the source  $S$  and receiver  $\psi$  becomes

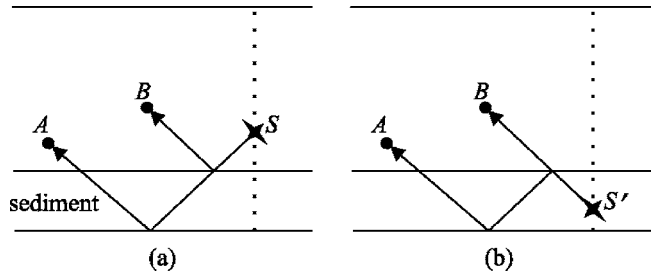


FIG. 3. Example of (a) water source and (b) sediment source stationary points that cancel with one another and do not contribute to the Green's function.

$$L_\psi = \sqrt{x_\psi^2 + \left( 2pD + \sum_{m=1}^M (2q_m D_{sm}) \pm z \pm z_\psi \right)^2}, \quad (16)$$

where  $p$  and  $q_m$  are the multiple order in the water and each sediment layer  $m$ , and  $D_{sm}$  is the depth of the  $m$ th sediment layer. The stationary phase condition is still  $\phi_A = \phi_B$ ; however, there exist paths satisfying this condition whose path length differences are not identical to any component lengths of the Green's function between the two receivers. For example, in Fig. 3(a) the path to receiver  $B$  is a reflection from the sediment-water interface. The path to receiver  $A$  is a transmission through this interface, a reflection from the basement, and a transmission back into the water. The stationary phase condition of  $\phi_A = \phi_B$  is satisfied; however, the path length difference is

$$L = \sqrt{x_A^2 + (2D + 2D_s - z - z_A)^2} - \sqrt{x_B^2 + (2D - z - z_B)^2}, \quad (17)$$

which, in general, differs from the path length of any wave that travels between the two receivers, and therefore should not contribute to the Green's function. Note that the path length difference and hence the time at which these spurious arrivals occur is dependent on the horizontal distance separating the source column from the receivers. If the column of sources were extended into the sediment, a second stationary point of equal amplitude and opposite phase would exist [see Fig. 3(b)], canceling the contribution of the water-source stationary point.

Note that Eq. (13) contains a  $\rho_s^2$  term, but pressure is proportional to  $\rho_s G_f$ , and hence the individual cross-correlations need to be normalized by the density at the source location before summing. More complex paths may exhibit multiple stationary points, located in both the water column and the sediment, corresponding to a particular path length difference; however, they will sum to zero so long as the source column spans all paths that have a stationary point.

Introduction of a varying sound speed profile will further complicate the problem; however, OAI is still applicable. Snieder *et al.* (Appendix A)<sup>24</sup> present work that generalizes their arguments for the direct wave in a homogeneous medium to a direct wave in a heterogeneous medium with variations in velocity that are sufficiently smooth for ray theory to remain applicable. The environment and geometry used here are different from that of Snieder *et*

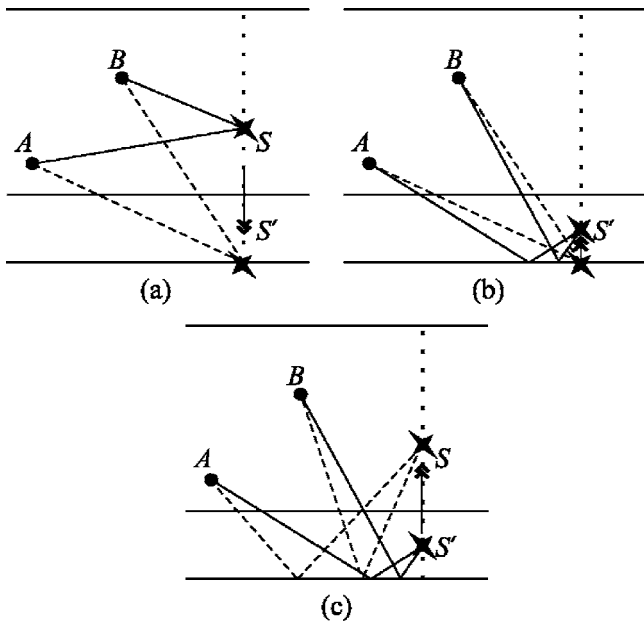


FIG. 4. The direct path (a) and bottom bounce path [dashed line in (c)] are linked via a continuous transition through sediment source configurations (a)–(c); a truncation of the integral results in a discontinuity in the arrival structure of the paths if sediment sources are not considered.

*al.*; however, the idea of generalizing from a homogeneous to a heterogeneous medium is the same. The inclusion of attenuation will also add complications since it will generally result in the paths not canceling exactly; the degree to which they will cancel one another is environment dependent.

Truncations in the integral of Eq. (15) may also be apparent as peaks in the summed cross-correlation at time intervals corresponding to correlations between paths from sources located at the water-sediment interface. Consider, as an example, the paths depicted in Figs. 4(a)–4(c). As the source is moved towards the water-sediment interface, the direct paths [solid line in Fig. 4(a)] converge to the direct paths from a source in the sediment [dashed line in Fig. 4(a)]. At the bottom of the sediment these paths converge with the bottom bounce paths [solid line in Fig. 4(b)], which in turn converge to the dashed path shown in Fig. 4(c) at the water-sediment interface. If the sources in the sediment are not included in the summation, discontinuities in the integral will exist at the water-sediment interface for the water source paths in both Figs. 4(a) and 4(c). The path length difference for this discontinuity is

$$\Delta L = \sqrt{(D - z_A)^2 + x_A^2} - \sqrt{(D - z_B)^2 + x_B^2} - \left( \sqrt{(D - z_A + 2D_s)^2 + x_A^2} - \sqrt{(D - z_B + 2D_s)^2 + x_B^2} \right), \quad (18)$$

where  $D_s$  is the depth of the sediment. If the sediment is shallow ( $D_s \ll D$ ), these discontinuities may not be observable in the summed cross-correlations since the path length differences for a source at the sediment-water interface will be small; however, if the sediment is deep, the discontinuity may be observed as two distinct spurious peaks separated temporally by  $\Delta L/c$ .

Restricting the sources to the water column can therefore lead to spurious peaks in the cross-correlation function. If the sources are extended through the sediment and the cross-correlation function is normalized by the density at the source, these spurious peaks may be avoided.

In a generalized environment, the mathematics becomes more complex; however, the fundamental ideas hold. An amplitude and  $3\pi/4$  phase shaded Green's function will still be obtained by summing the density normalized source cross-correlations, so long as the source column spans the water column and all underlying sediments. The effect of limiting the sources to the water column, upon the similarity between the summed cross-correlations and the shaded Green's function, is environment dependent.

### C. Spurious arrivals

Snieder *et al.*<sup>24</sup> and Sabra *et al.*<sup>12</sup> determined that spurious arrivals also exist for their particular geometries and environments. The spurious arrivals that they discuss and the ones described here are all due to the volume of interest not being fully enclosed by sources; however, each of these aberrations is distinct.

The spurious arrivals described in Sec. II B occur when the sources are limited to the water column. The integral does not extend to infinity, resulting in two causes of spurious arrivals. As the source approaches the upper and lower boundaries (surface and basement), different paths will converge. Hence, when the sources are contained to the water column, paths that would converge at the sediment bottom do not converge. Spurious peaks therefore occur at these path discontinuities. The second mechanism of spurious arrivals is a stationary-phase contribution from a source in the water column that does not actually contribute to the full Green's function. This contribution occurs from correlations between waves that are reflected at the water-sediment interface and waves that pass into the sediment. It should cancel with a stationary-phase contribution of equal amplitude and opposite phase from the sediment and therefore a false peak is recorded when sediment sources are not included.

Sabra *et al.*<sup>12</sup> modeled time-averaged surface generated ambient noise using a horizontal plane of point sources at a constant depth in a waveguide. The spurious arrivals they described are caused by stationary-phase contributions from correlations between a wave that initially undergoes a surface reflection and one that does not (for an isovelocity water column, one wave departs at an angle of  $\phi$  from the horizontal, and the other departs at an angle of  $-\phi$ ). These stationary points are intrinsic to the horizontal source configuration. If the depth of the plane of sources is reduced, the spurious peaks converge to the same time delay as the true Green's function paths; however, they are  $\pi$  out of phase and will still result in shading of the Green's function.

Snieder *et al.*<sup>24</sup> used a horizontal line of evenly spaced sources in a homogeneous medium, with one or more horizontal reflectors below and no free surface above. Snieder's assumption of there being no free surface means that the spurious paths described by Sabra *et al.* did not exist in their analysis. The spurious arrivals described by Snieder *et al.* are

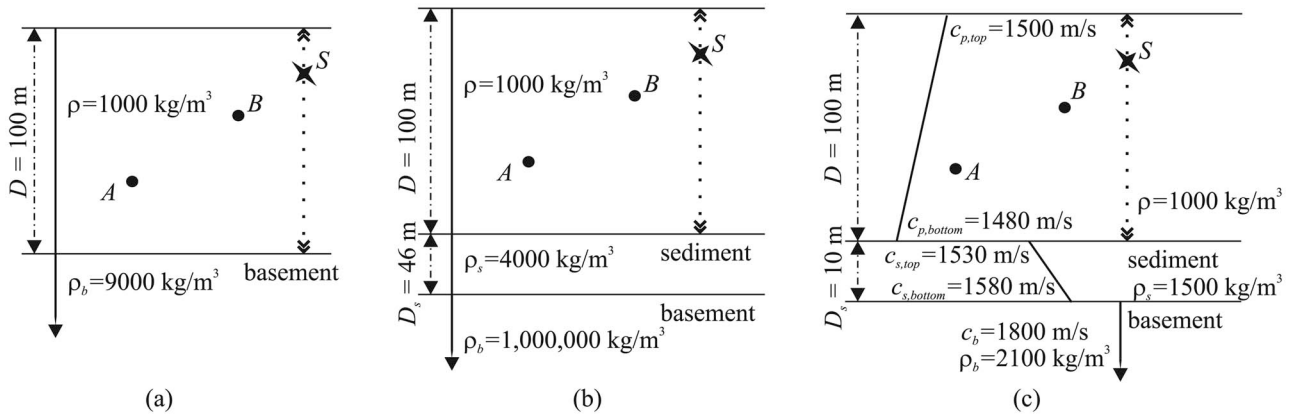


FIG. 5. Simulated waveguide environments: (a) isovelocity waveguide with a purely reflective bottom (constant  $c=1500$  m/s), (b) isovelocity purely reflective waveguide with a sediment layer (constant  $c=1500$  m/s), and (c) more realistic refractive environment with a sediment layer.

due to false stationary-phase contributions caused by correlation of waves reflected from distinct reflectors, which occur due to the sources only being in the upper layer. To eliminate these spurious multiples, a second surface of sources would have to be included below the bottom reflector.

### III. SIMULATIONS

Three simulation environments were selected to clearly demonstrate application of OAI from a physical perspective. The Green's function between two receivers is approximated using the OAI approach for a vertical line of sources. Oases<sup>28</sup> was used for both the OAI approach and to compute the true Green's function between the receivers. The theory derived via the method of stationary phase in Sec. II is used only for discussion purposes.

The environments, depicted in Fig. 5, comprise (a) an isovelocity waveguide with a purely reflective bottom, (b) a completely reflective environment comprising an isovelocity waveguide and an isovelocity sediment layer, and (c) a more realistic environment with a downward refractive sound speed profile (SSP) waveguide, and an upward refractive SSP sediment layer. Receivers *A* and *B* are located at depths of 80 and 50 m, respectively. The two receivers are separated 100 m horizontally. A column of sources, spaced at 0.5-m increments, spans the water column in the same vertical plane as the two receivers, 40 m to the right of receiver *B*. The source is a Ricker wavelet with a center frequency of 350 Hz.

The sum of the cross-correlations, Eq. (1), is evaluated by treating the integral as a sum over the source column. For each source location, the acoustic pressure at *A* and *B* is evaluated assuming a constant source spectrum of  $S(\omega)$ . The pressures are cross-correlated, normalized by the density at the source, and then summed over the source locations and compared to the frequency and phase shaded Green's function between the two receivers:

$$\frac{\rho |S(\omega)|^2}{\omega} e^{i(3\pi/4)} G(R). \quad (19)$$

#### A. Isovelocity waveguide

The unstacked cross-correlations and the stacked response,  $C$ , are depicted in Fig. 6(a). The true  $[3\pi/4$  phase and  $|S(\omega)|^2$  amplitude] shaded simulated Green's function,  $G$ , is also included for comparative purposes.

The direct path stationary point is the temporal maxima of the direct wave cross-correlation arrival structure to each receiver. It occurs at 38-m depth at a time of 0.070 s. The direct path time difference converges to 0.065 s as the source is moved towards the surface, and to 0.052 s as it is moved towards the bottom. These endpoints do not, however, result in spurious peaks in the stacked response as they converge with other paths as the source approaches the given boundary. Stationary points corresponding to arrivals of the reflected paths are more difficult to see as they occur at locations very close to the waveguide boundaries; however, they can still be seen in the stacked response. For example, the peak in the stacked correlations at 0.109 s corresponds to the stationary point of the bottom bounce path to receiver *B* and the bottom-surface bounce path to receiver *A*, which occurs at a depth of 98 m and is therefore difficult to distinguish.

Overall, the phase of the stacked cross-correlation shows good agreement with the frequency and phase shaded Green's function, with only minor deviations. The amplitude is not accurate, but this can be explained by the difference in amplitude between the stacked cross-correlations and the Green's function having path dependent components ( $\Gamma^{b_A+b_B}$ ,  $\phi_s$ , and  $\xi$ ) as derived in Eq. (13).

#### B. Waveguide with single sediment layer

This particular waveguide environment was chosen in order to understand a means by which the stacked cross-correlations may show some differences from the shaded simulated Green's function. In order to emphasize what is happening, the receivers are separated only 30 m horizontally, the Ricker wavelet centre frequency has been doubled to 700 Hz, and the source column spacing halved to 0.25 m. The remainder of the source/receiver configuration is identical to that of the isovelocity waveguide example.

The unstacked cross-correlations and the stacked responses are depicted in Fig. 6(b). The stacked response  $\Sigma C$

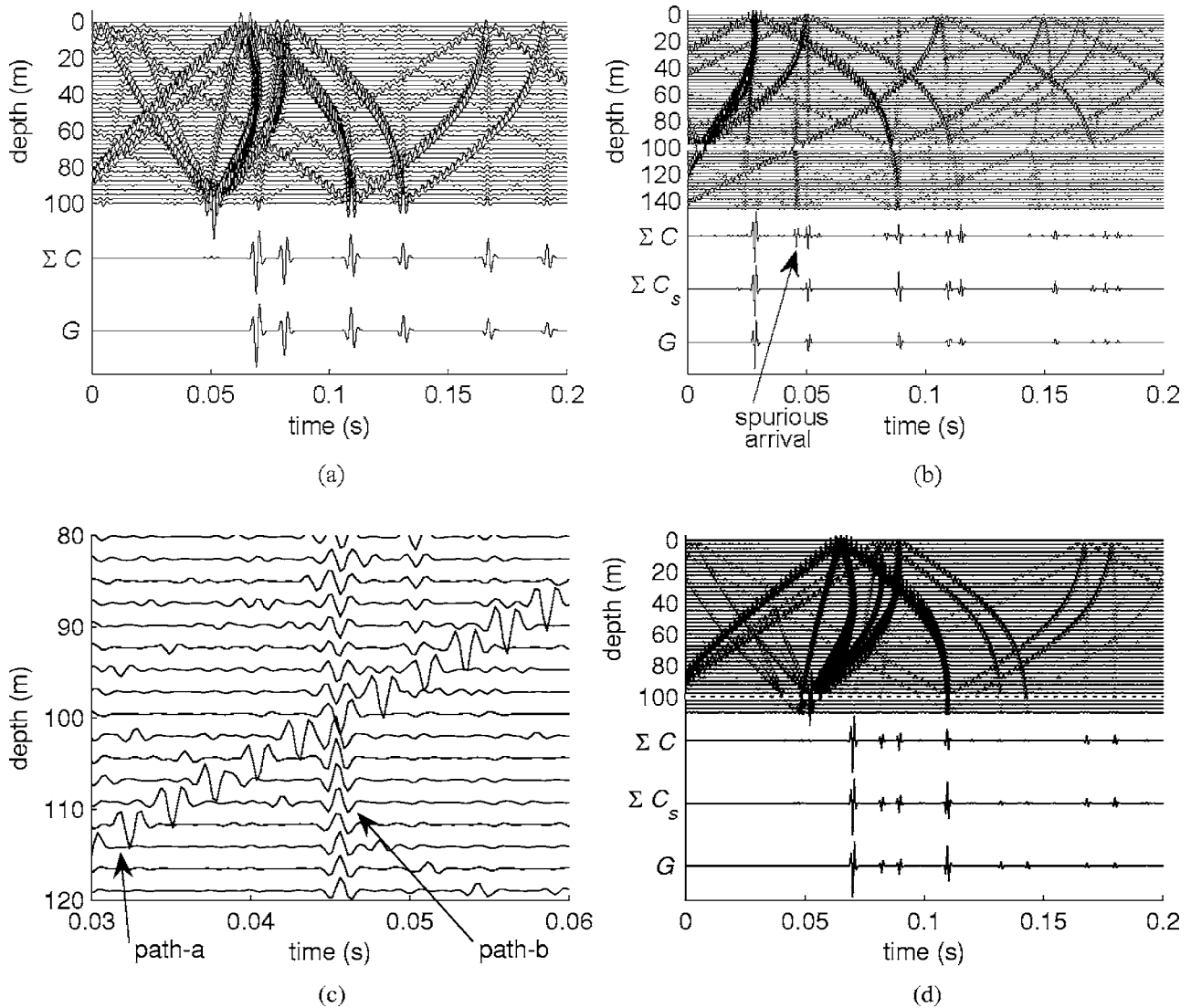


FIG. 6. The cross-correlations for (a) the isovelocity waveguide, (b) the reflective environment with a sediment, (c) a magnified portion of (b), and (d) the refractive environment, are plotted as a function of depth. The water-sediment interfaces in (b) and (d) are marked by a dashed white line. The stacked cross-correlation from a column of sources in the water,  $\Sigma C$ , the stacked trace with sediment sources included [(b) and (d) only],  $\Sigma C_s$ , and the shaded Green's function,  $G$ , are also plotted. The two paths indicated in (c) are the arrivals for the ray paths depicted in Fig. 7.

for the case when the source column terminates at the water-sediment interface contains the arrival paths observable in the shaded Green's function  $G$ ; however, it also contains several spurious arrivals, the most noticeable of which occurs within the time interval 0.044–0.047 s. The stacked response  $\Sigma C_s$  does not contain these spurious arrivals. The spurious arrivals observable in  $\Sigma C$  are due to the source column not continuing through the sediment and therefore not producing a perfect time-reversal mirror.

One contribution to this spurious arrival is due to the discontinuities in the arrival structure caused by truncation of the  $C_{AB}(\omega)$  integral at the bottom of the water column. The two paths affected are shown in Figs. 7(a) and 7(b) and their cross-correlations, depicted in Fig. 6(c), are denoted path-a and path-b, respectively. Paths-a and -b are cross-correlation peaks and, as such, should not be confused with real arrivals. As the source approaches the water-sediment interface the arrival time for path-a, the solid line in Fig. 7(a), transitions smoothly with the solid line, path-b, of Fig. 7(b). This can be

seen by examining the arrival structure in Fig. 6(c). The two arrivals do not, however, cancel each other. For both paths-a and -b the path length difference between the source and

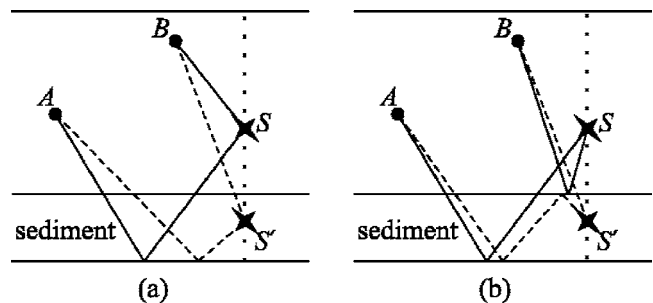


FIG. 7. Two possible sets of ray paths: (a) direct path to  $B$  and the bottom bounce path to  $A$ , and (b) a path to  $B$  with one water-sediment bounce and a path to  $A$  that has two transmissions through the interface. In both cases the solid lines represent paths from sources in the water (denoted  $S$ ) and the dashed lines represent paths from sources in the sediment (denoted  $S'$ ).

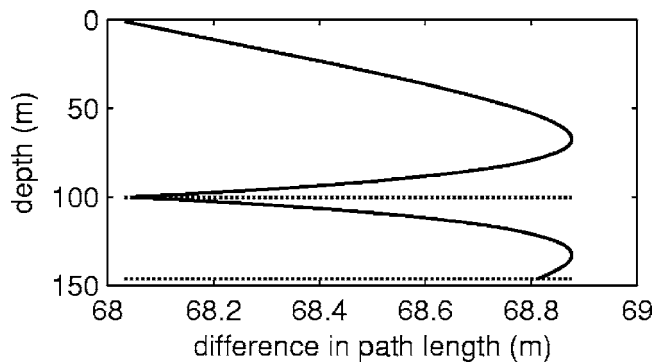


FIG. 8. The difference between the path lengths from the source to receiver *A* and the source to receiver *B* as a function of source depth for the ray path geometry of Fig. 7(b). The horizontal dotted lines represent the water-sediment interface and the sediment bottom.

each receiver decreases as the source approaches the sediment [see Figs. 6(c) and 8]. The two sets of ray paths are also in phase [see Fig. 6(c)]. The two arrivals will therefore sum together to contribute to the largest spurious arrival in trace  $\Sigma C$  of Fig. 6(b).

If the sources are extended through the sediment to the basement, then the summation over the arrival structure corresponding to Fig. 7 cancels completely at the water-sediment interface. At the interface the cross-correlation of the solid line representation of path-a [see Fig. 7(a)] will transition smoothly into the dashed line representation of path-a both in terms of arrival time and amplitude (for path  $A+B$  the number of transmissions through the sediment remains constant). The difference in path length has a local minima here (see Fig. 8); however, the phase of the cross-correlation is inverted at the interface [see Fig. 6(c)], resulting in direct cancellation. Path-b also transitions smoothly; however, this time the difference in path length continues to decrease and there is no phase change [see Fig. 6(c)]. Cancellation at the interface therefore occurs. As the source approaches the basement, the arrival structure and amplitude will transition smoothly into that of other paths. For example, path-a will converge to the same arrival time as all other combinations of direct and single basement bounce paths to *A* and *B*, and, since the amplitudes of each set of paths will be the same, a smooth transition between the paths will occur.

A second contribution to the largest spurious arrival is a stationary-phase contribution from a source in the water column, which does not actually contribute to the full Green's function, as explained in Fig. 3. The solid line of path-b should not contribute to the Green's function as the signal received by *A* never passes through *B*, regardless of the source depth; however, a stationary point exists when the two paths depart the source at the same angle (i.e., 67.3 m source depth). This stationary point is difficult to see in the stacked response since the difference in path length of Fig. 7(b) varies by less than a meter ( $\sim \lambda/5$ ) over the entire depth (see Fig. 8). As seen in Fig. 8, a second stationary point exists within the sediment at a depth of 133 m. If the sources are extended through the sediment, then this stationary point annuls the contribution from the stationary point in the water column.

As expected, the largest spurious peak from the water source column cross-correlation is not observable in the stacked cross-correlation of the column of sources that extends through the sediment [see trace  $\Sigma C_s$  of Fig. 6(b)]. Other deviations from the expected shaded Green's function are also reduced or removed.

### C. Refractive environment with sediment

The source and receiver geometry and source type are identical to that of the (original) isovelocity waveguide example. The stacked responses,  $\Sigma C$  (sources in water column only) and  $\Sigma C_s$  (sources extended through sediment), and the shaded Green's function  $G$  are shown in Fig. 6(d). The phase of the water column stacked response is in reasonable agreement with the shaded simulated Green's function. The path time differences have converged almost completely to their sediment-bottom interface value at the water-sediment interface and hence the spurious arrivals, which were easily observed in the previous example, are not apparent here. Even if the source column could be extended into the sediment, only a minor increase in accuracy would be obtained. These results agree with the simulations of Roux and Fink,<sup>23</sup> who concluded that the effect of limiting sources to the water column is negligible when the modal continuum of the sediment is small relative to that of the water.

## IV. CONCLUSION

Ocean acoustic interferometry (OAI) refers to the process of recording the signals from a line of sources on two receivers and using this to infer the Green's function between the receivers. The time domain Green's function is approximated by summing or integrating, over all source positions, the cross-correlations between the receivers. The source used in this work was a vertical (drop) source spanning the water column; however, the source could also have been a horizontal (tow) source.

Analytical stationary phase based OAI was used to solve the summation of cross-correlations for a line of vertical sources, located external to, and in the same plane as, two receivers, and to relate this to the Green's function between said receivers. It was shown that in an isovelocity waveguide, the stacked cross-correlations show very good agreement with the  $|S(\omega)|^2/\omega$  amplitude, and  $3\pi/4$  phase, shaded Green's function.

Numerical simulations of OAI were used to confirm the theoretical findings and also to show what can happen in a more complex environment. A concern is that the introduction of a sediment can produce, in addition to arrivals pertaining to the true time domain shaded Green's function, spurious arrivals due to the sources ceasing at the water-sediment interface. The origin of these spurious arrivals was discussed in detail. These aberrations can, theoretically, be removed by extending the line of sources into the sediment.

In the refractive environment presented here the phase of the water column stacked response  $\Sigma C$  was shown to be in reasonable agreement with the shaded simulated Green's function  $G$ ; however, the extent to which  $\Sigma C$  and  $G$  agree is environmentally dependent. If the modal continuum of the

sediment were higher relative to that of the water, differences between  $\Sigma C$  and  $G$  would be more prevalent.

In an experimental setting the vertical source column source/receiver geometry could be achieved using a source that is slowly lowered through the water by a ship-operated winch, and by recording data on either two vertical arrays or an L-shaped array. One application for this could be monitoring changes in the ocean environment between two arrays.

## ACKNOWLEDGMENTS

This work was supported by the Office of Naval Research under Grant No. N00014-05-1-0264. The first author is also appreciative of support from a Fulbright Postgraduate Award in Science and Engineering, sponsored by Clough Engineering, as well as support from the Defence Science and Technology Organisation, Australia.

- <sup>1</sup>O. I. Lobkis and R. L. Weaver, "On the emergence of the Green's function in the correlations of a diffuse field," *J. Acoust. Soc. Am.* **110**, 3011–3017 (2001).
- <sup>2</sup>A. Derode, E. Larose, M. Tanter, J. de Rosny, A. Tourin, M. Campillo, and M. Fink, "Recovering the Green's function from field-field correlations in an open scattering medium," *J. Acoust. Soc. Am.* **113**, 2973–2976 (2003).
- <sup>3</sup>K. Wapenaar, "Retrieving the elastodynamic Green's function of an arbitrary inhomogeneous medium by cross correlation," *Phys. Rev. Lett.* **93**, 254301 (2004).
- <sup>4</sup>D.-J. van Manen, J. O. A. Robertsson, and A. Curtis, "Modeling of wave propagation in inhomogeneous media," *Phys. Rev. Lett.* **94**, 164301 (2005).
- <sup>5</sup>F. J. Sánchez-Sesma and M. Campillo, "Retrieval of the Green function from cross correlation: The canonical elastic problem," *Bull. Seismol. Soc. Am.* **96**, 1182–1191 (2006).
- <sup>6</sup>F. J. Sánchez-Sesma, J. A. Pérez-Ruiz, M. Campillo, and F. Luzón, "Elastodynamic 2D Green function retrieval from cross-correlation: Canonical inclusion problem," *Geophys. Res. Lett.* **33**, L13305 (2006).
- <sup>7</sup>R. L. Weaver and O. I. Lobkis, "Ultrasonics without a source: Thermal fluctuation correlations at MHz frequencies," *Phys. Rev. Lett.* **87**, 134301 (2001).
- <sup>8</sup>A. E. Malcolm, J. A. Scales, and B. A. van Tiggelen, "Extracting the Green function from diffuse, equipartitioned waves," *Phys. Rev. E* **70**, 015601 (2004).
- <sup>9</sup>K. van Wijk, "On estimating the impulse response between receivers in a controlled ultrasonic experiment," *Geophysics* **71**, SI79–SI84 (2006).
- <sup>10</sup>P. Roux, K. G. Sabra, W. A. Kuperman, and A. Roux, "Ambient noise cross correlation in free space: Theoretical approach," *J. Acoust. Soc. Am.* **117**, 79–84 (2005).
- <sup>11</sup>P. Roux, W. A. Kuperman, and the NPAL Group, "Extracting coherent wave fronts from acoustic ambient noise in the ocean," *J. Acoust. Soc. Am.* **116**, 1995–2003 (2004).
- <sup>12</sup>K. G. Sabra, P. Roux, and W. A. Kuperman, "Arrival-time structure of the time-averaged ambient noise cross-correlation function in an oceanic waveguide," *J. Acoust. Soc. Am.* **117**, 164–174 (2005).
- <sup>13</sup>K. G. Sabra, P. Roux, A. M. Thode, G. L. D'Spain, W. S. Hodgkiss, and W. A. Kuperman, "Using ocean ambient noise for array self-localization and self-synchronization," *IEEE J. Ocean. Eng.* **30**, 338–347 (2005).
- <sup>14</sup>M. Siderius, C. H. Harrison, and M. B. Porter, "A passive fathometer technique for imaging seabed layering using ambient noise," *J. Acoust. Soc. Am.* **120**, 1315–1323 (2006).
- <sup>15</sup>M. Campillo and A. Paul, "Long-range correlations in the diffuse seismic coda," *Science* **299**, 547–549 (2003).
- <sup>16</sup>R. Snieder, "Extracting the Green's function from the correlation of coda waves: A derivation based on stationary phase," *Phys. Rev. E* **69**, 046610 (2004).
- <sup>17</sup>N. M. Shapiro, M. Campillo, L. Stehly, and M. H. Ritzwoller, "High-resolution surface-wave tomography from ambient seismic noise," *Science* **307**, 1615–1618 (2005).
- <sup>18</sup>K. G. Sabra, P. Gerstoft, P. Roux, W. A. Kuperman, and M. C. Fehler, "Extracting time-domain Green's function estimates from ambient seismic noise," *Geophys. Res. Lett.* **32**, L03310 (2005).
- <sup>19</sup>P. Gerstoft, K. G. Sabra, P. Roux, W. A. Kuperman, and M. C. Fehler, "Green's functions extraction and surface-wave tomography from microseisms in southern California," *Geophysics* **71**, S123–S131 (2006).
- <sup>20</sup>K. Wapenaar and J. Fokkema, "Green's function representations for seismic interferometry," *Geophysics* **71**, SI33–SI46 (2006).
- <sup>21</sup>J. Rickett and J. Claerbout, "Acoustic daylight imaging via spectral factorization; helio-seismology and reservoir monitoring," *The Leading Edge* **18**, 957–960 (1999).
- <sup>22</sup>E. Larose, A. Khan, Y. Nakamura, and M. Campillo, "Lunar subsurface investigated from correlation of seismic noise," *Geophys. Res. Lett.* **32**, L16201 (2005).
- <sup>23</sup>P. Roux and M. Fink, "Green's function estimation using secondary sources in a shallow water environment," *J. Acoust. Soc. Am.* **113**, 1406–1416 (2003).
- <sup>24</sup>R. Snieder, K. Wapenaar, and K. Larner, "Spurious multiples in seismic interferometry of primaries," *Geophysics* **71**, SI111–SI124 (2006).
- <sup>25</sup>A. Curtis, P. Gerstoft, H. Sato, R. Snieder, and K. Wapenaar, "Seismic interferometry—turning noise into signal," *The Leading Edge* **25**, 1082–1092 (2006).
- <sup>26</sup>L. M. Brekhovskikh, *Waves in Layered Media* (Academic, New York, 1960).
- <sup>27</sup>C. M. Bender and S. A. Orszag, *Advanced Mathematical Methods for Scientists and Engineers* (McGraw-Hill, New York, 1978).
- <sup>28</sup>H. Schmidt, *OASES Version 3.1 User Guide and Reference Manual*, Department of Ocean Engineering, Massachusetts Institute of Technology (2004).